Journal of Drug Delivery Science and Technology 99 (2024) 105972

Contents lists available at ScienceDirect

Journal of Drug Delivery Science and Technology

journal homepage: www.elsevier.com/locate/jddst

Characterization of PLGA versus PEG-PLGA intracochlear drug delivery implants: Degradation kinetics, morphological changes, and pH alterations

Eric Lehner [a,f,*], Arne Liebau [a], Matthias Menzel [b], Christian E.H. Schmelzer [b,c], Wolfgang Knolle [d], Jonas Scheffler [a], Wolfgang H. Binder [e], Stefan K. Plontke [a,f], Karsten Mäder [c,f]

[a] Department of Otorhinolaryngology-Head and Neck Surgery, Martin Luther University Halle-Wittenberg, Ernst-Grube-Straße 40, 06120, Halle (Saale), Germany
[b] Fraunhofer Institute for Microstructure of Materials and Systems IMWS, Walter-Hülse-Straße 1, 06120, Halle (Saale), Germany
[c] Institute of Pharmacy, Martin Luther University Halle-Wittenberg, Wolfgang-Langenbeck-Straße 4, 06120, Halle (Saale), Germany
[d] Leibniz Institute of Surface Engineering (IOM), Permoserstraße 15, 04318, Leipzig, Germany
[e] Institute of Chemistry, Martin Luther University Halle-Wittenberg, Von-Danckelmann-Platz 4, 06120, Halle (Saale), Germany
[f] Halle Research Centre for Drug Therapy (HRCDT), Halle (Saale), Germany

ARTICLE INFO

Keywords:
Polymer degradation
Intracochlear
Dexamethasone
Hot-melt extrusion
PEG-PLGA
Inner ear drug delivery

ABSTRACT

Drug delivery to the inner ear presents a unique challenge due to the complex inner ear anatomy and its tight physiological barriers. This study investigates the degradation behavior of intracochlear drug delivery implants (IDDI) composed of dexamethasone and poly(lactic-*co*-glycolic acid) (PLGA) or polyethylene glycol–poly(lactic-*co*-glycolic acid) (PEG-PLGA), respectively. IDDI were incubated in artificial perilymph and implants' degradation kinetics, morphological changes, water uptake behavior, and pH alterations were assessed. Microscopy revealed significant changes in appearance, with PLGA IDDI exhibiting rapid expansion, reaching up to 183 % in diameter and 185 % in length. PEG-PLGA implants showed gradual expansion, reaching a maximum of 178 % in diameter and 144 % in length. Despite these morphological changes, the IDDIs could still be applicable in terms of cochlear dimensions in combination with cochlear implants (CI) in humans or in a domestic pig animal model. Scanning electron microscopy analysis demonstrated surface alterations of PLGA implants, while PEG-PLGA implants remained shape-stable. Gravimetric analysis and gel permeation chromatography revealed distinct degradation profiles, with PLGA implants displaying rapid water uptake and mass loss, while PEG-PLGA implants showed delayed water uptake and minimal mass reduction. pH measurements using the pH-sensitive fluorescent dye SNARF™-1 showed initial pH reduction in artificial perilymph for PLGA implants while PEG-PLGA implants maintained pH stability.

1. Introduction

Local drug delivery to the inner ear remains an unmet medical need due to the limited access of systemic therapy caused by the tight blood-labyrinth barrier [1]. This barrier necessitates high systemic doses, which can lead to side effects or exposure to first-pass effects [2–5]. Overcoming these limitations, local drug release to the inner ear offers several advantages, including bypassing the blood-labyrinth barrier, avoiding "first-pass" metabolism, and reducing overall dosage. The currently most employed method is extracochlear drug delivery by intratympanic injection of a drug solution or (thermo-)gel formulation through the tympanic membrane into the middle ear. The drug then diffuses through the inner ear windows (mainly the round window membrane, RWM) into the inner ear. Primary obstacles for extracochlear drug delivery include mucosal obstructions of the RWM, the rapid removal of the drug from the middle ear, and the diffusion barriers presented by the multilayer RWM or the oval window [1,6,7]. Polymer-based systems have been investigated preclinically for sustained drug delivery via extracochlear administration [8–12]. However, intracochlear drug delivery, in which the drug is directly released into the inner ear fluid, overcomes the limitations of both, systemic and extracochlear drug delivery [13]. Currently, intracochlear drug delivery

* Corresponding author. Martin Luther University Halle-Wittenberg Department of Otorhinolaryngology-Head and Neck Surgery, Ernst-Grube-Straße 40, 06120, Halle (Saale), Germany.
E-mail address: eric.lehner@uk-halle.de (E. Lehner).

https://doi.org/10.1016/j.jddst.2024.105972
Received 14 May 2024; Received in revised form 9 July 2024; Accepted 11 July 2024
Available online 18 July 2024

with controlled release characteristics is primarily associated with drug-eluting electrode carriers of cochlear implants (CI) [14–18]. Cochlear implants are well established to treat patients with profound hearing loss or partial deafness with residual low frequency hearing. However, foreign body response (FBR) against the electrode carrier may result in formation of connective tissue (fibrosis) and ossification. Fibrosis leads to an impairment of the neural interface with increased impedances and in some patients to balance disorders and makes cochlear reimplantation difficult or impossible. Fibrosis also causes progressive loss of residual hearing by increasing the basilar membrane stiffness. Considering the increased demand for cochlear implantation and the expansion of the clinical indications for the recipients, fibrosis is one of the most urgent problems to be solved to improve the outcomes of cochlear implantation. Clinical pilot studies demonstrated inhibition of the FBR in the inner ear after cochlear implantation when using glucocorticoids [18,19]. However, promising approaches also exist without neuroprosthetic devices [20,21]. Our previous work focused on developing biodegradable, intracochlear drug delivery implants (IDDI) [22,23]. The mechanical properties and drug release profiles were controlled by adjusting the polymer matrix and incorporating plasticizers. We demonstrated the overall feasibility of administering PLGA implants into the scala tympani of the human inner ear and co-administering them with a CI electrode array [24]. However, there is limited understanding regarding the degradation of these IDDI, particularly those that are based on PEG-PLGA. Generally, PEG-PLGA polymers prevent the formation of an acidic microenvironment and exhibit uniform polymer degradation [25–27]. However, there is no data available for preformed implants with a very small diameter of approximately 300 μm. The size of implants plays a crucial role in determining their degradation characteristics, including water uptake, mass loss, and polymer degradation [28].

This study provides insights into the degradation kinetics and morphological changes of IDDI, crucial for upcoming *in vivo* studies. Light microscopy and scanning electron microscopy were used to observe IDDI morphology. Gravimetric analysis and gel permeation chromatography (GPC) were utilized to quantify the extent of degradation. Differential scanning calorimetry (DSC) analysis provided insights into the glass transition temperatures, explaining the thermal characteristics of the IDDI materials. Additionally, the use of SNARF-1 dye facilitated the measurement of pH changes in artificial perilymph, offering information about the environmental conditions surrounding the IDDI.

2. Material and methods

2.1. Materials

Expansorb® polymer 10P019 DLG 50-2A (poly(lactic-*co*-glycolic acid); PLGA) was obtained from Merck KGaA (Darmstadt, Germany). Expansorb® 10P037 DLG 50-6P (polyethylene glycol–poly(lactic-*co*-glycolic acid); PEG-PLGA) was purchased from Seqens (Ecully Cedex, France). Dexamethasone was bought from Caesar & Loretz GmbH (Hilden, Germany). Polyethylene glycol (PEG) 1500 was purchased from Alfa Aesar (Haverhill, USA). The fluorescence dye SNARF-1 (5-(and-6)-Carboxy SNARF™-1) was purchased from Invitrogen (Darmstadt, Germany). Artificial perilymph consisting of NaCl (137 mM), KCl (5 mM), $CaCl_2$ (2 mM), $MgCl_2$ (1 mM), $NaHCO_3$ (1 mM), and glucose (11 mM) was used. To avoid microbial growth, sodium azide 0.02 % was added to artificial perilymph. All other chemicals were used without further purification. Aqueous solutions were prepared using deionized water.

2.2. Implant preparation using hot-melt extrusion

PLGA and PEG-PLGA were milled in a Cryomill (Retsch GmbH, Haan, Germany) for 90 s at 4 cycles with a frequency of 25 Hz. Subsequently, precise quantities of pulverized polymer and dexamethasone underwent a second milling for 90 s at 15 Hz, followed by extrusion utilizing a ZE 5 ECO extruder equipped with a 0.3 mm die (ZE 5 ECO; Three-Tec GmbH; Seon; Swiss). For PLGA-based implants, PEG 1500 was added during the second milling stage at concentrations of 10 % (Table 1). A comprehensive description of this process can be found in our prior study [23]. Following extrusion, the hot-melt extrudates were manually cut into pieces weighing 1 mg or measuring 3 mm in length and stored at −20 °C.

2.3. Electron beam irradiation

The selected sterilization process utilized electron beam irradiation. The extruded material underwent irradiation at room temperature. The dose administered was 25 kGy, delivered by a 10 MeV linear accelerator (MB 10–30 MP, Mevex, Stittsville, Ontario, Canada) on a moving tray at 95 cm/min. The accelerator operated at a repetition rate of 460 Hz, generating 8 μs pulses, and employed a scanning frequency of 3 Hz with a scanning width of up to 60 cm. The total dose of 25 kGy was achieved through the administration of two separate doses of 12.5 kGy.

2.4. Macroscopic examination

IDDI of 3 mm length (n = 3) were incubated in 1 ml artificial perilymph in 12-well cell culture plates. Samples were maintained at 37 °C in a shaker incubator at 25 rpm (Heidolph Promax 1020 coupled with Heidolph Incubator 1000, Schwabach, Germany). Microscopic images of the IDDI in wet condition were captured for 90 days using a Zeiss Axio Zoom.V16 microscope. Lengths and diameters of the IDDI were determined using Zen 3.1 software (Carl Zeiss, Oberkochen, Germany). Artificial perilymph was refreshed nearly every day, with the latest replacement occurring no later than every 3 days.

2.5. Scanning electron microscopy (SEM)

The morphological analysis of the sample series was conducted using a Quanta 3D FEG scanning electron microscope (FEI Company, Eindhoven, Netherlands). Samples were incubated as described in section 2.4. and removed after 3, 7, 14, 21, and 28 days. Afterwards, the samples were washed with double-distilled water to remove buffer salt crystals from the surface. IDDI were then dried in a desiccator under vacuum for 48 h. After drying, the samples were immobilized onto an adhesive carbon conduction tab (Plano® Carbon, Plano GmbH, Wetzlar, Germany) and sputtered with palladium for adequate conductivity. For imaging, accelerating voltages ranging from 2 to 5 keV and beam currents varying between 22 and 57 pA were used as required, with the secondary electron signal recorded.

2.6. Differential scanning calorimetry (DSC)

DSC measurements were conducted using a Mettler Toledo DSC 823e module (Mettler Toledo, Gieβen, Germany) with standard aluminum sample pans. 10 mg of each implant formulation was incubated as described in 2.4. After 3, 7, 14, 21, and 28 days, IDDI were taken out carefully, blotted with tissue and dried in a desiccator under vacuum for 48 h. Each sample was initially cooled to −38 °C and maintained at this temperature for 4 min. Then, samples were heated to 80 °C at a rate of 5 K/min. The software STARe V15.00 (Mettler Toledo, Gieβen, Germany) was employed for data recording and processing. Glass transition temperatures of first heating cycles are displayed.

Table 1
Composition of prepared IDDI (% m/m).

Implant name	PLGA	PEG-PLGA	PEG 1500	Dexamethasone
DEX-PLGA	80	–	10	10
DEX-PEG-PLGA	–	90	–	10

2.7. Implant degradation and water uptake

10 mg of each IDDI formulation were incubated as described in 2.4. After 3, 7, 14, 21, and 28 days, IDDI were withdrawn carefully, blotted with tissue, weighed (m_{wet}) and dried in a desiccator under vacuum for 48 h. The remaining mass (m_{dry}) of dried IDDI was determined by gravimetric analysis. The molecular weight of PLGA and PEG-PLGA was determined by a Viscotek GPCmax VE 2002 system (Malvern Panalytical GmbH, Kassel, Germany), consisting of $H_{HR}H$ Guard-17369 and GMH_{HR}-N-18055 columns and a refractive index detector VE 3580 RI, operated at 40 °C. Dried IDDI were dissolved in tetrahydrofuran (THF) to achieve concentrations of 3 mg/ml and subsequently filtered (PTFE-filters). The flow rate of the THF eluent was 1.0 mL/min, and polystyrene standards (PS) with a molecular weight range from 0.3 to 170 kg/mol (polydispersities <1.05) were used for calibration. Samples were filtered (0.22 μm) before measuring. The water uptake was calculated by Equation (1):

$$Water\ uptake\ [\%] = \frac{m_{wet} - m_{dry}}{m_{dry}} * 100\% \quad (1)$$

Artificial perilymph was refreshed daily until examination. Measurements were conducted in triplicate.

2.8. pH measurement using fluorescence microscopy

The change in pH of artificial perilymph containing biodegradable IDDI was assessed using fluorescence microscopy with the pH-sensitive dye SNARF-1. Depending on the type of SNARF dye utilized, the sensitivity of the dye allows for the detection of pH values in the range of pH 5 to 8 [29–31]. For each implant formulation, 1 mg of IDDI was incubated in 250 μL conical glass vial inserts filled with 100 μL of artificial perilymph. The inserts were then gently agitated in a water bath shaker with light protection (Memmert GmbH + Co. KG, Schwabach, Germany) at 37 °C. The total sample solution was withdrawn daily over a period of 28 days of incubation and analyzed. Prior to examination, 20 μL of SNARF-1 solution (40 μg/ml) was placed into a 100 μL conical glass vial insert and gently dried under vacuum conditions at 25 °C using a vacuum oven dryer (VG 53, Binder GmbH, Tuttlingen, Germany) attached with a NZ 2C NT vacuum pump (Vacuubrand, Wertheim am Main, Germany). Artificial perilymph samples were added to dried dye-containing vial inserts and investigated by multispectral fluorescence microscopy. Vials were placed under a fluorescence microscope consisting of a light source (PhotoFluor II NIR, 89 North®, Burlington, USA), a microscope (Leica DM4000B, Leica, Wetzlar, Germany) with a Nuance EX fluorescence detector (Nuance Communications, Burlington, USA). Two filter sets containing each a narrow band excitation filter and a longpass emission filter were used for the microscopic examination: green filter set (excitation filter, 515–560 nm; emission filter, 580 nm longpass, cube acquisition from 580 to 700 nm, 1 nm steps); red filter set (excitation filter, 620–660 nm; emission filter, 660 nm longpass; cube acquisition from 660 to 700 nm, 1 nm steps). The software (Nuance® 3.0.2) was used to calculate a cube that consists of a series of images taken at the specific wavelengths. For cube acquisition, automatic exposure tool was used for the green filter set to avoid over- or under-exposure. The exposure time for the red filter was manually set to the same value as for the green filter. Specific background spectrum was generated using untreated artificial perilymph. The ratio of intensities at I(606 nm) and I(680 nm) at green excitation light and I(682 nm) at red excitation light was calculated by Equation (2):

$$Ratio = \frac{I^{green}_{606\ nm} - I^{red}_{682\ nm}}{I^{green}_{680\ nm}} \quad (2)$$

The pH calibration was conducted using artificial perilymph containing 40 μg/ml SNARF-1, adjusted to different pH values ranging from 4.1 to 10.16 using NaOH and HCl.

3. Results and discussion

3.1. Morphological change during incubation

Observation of appearance and changes in diameter and length were conducted using light microscopy. IDDI were incubated in 12-well cell culture plates and imaged without removing. Careful handling was crucial, as otherwise, the implants would quickly fragment. Fig. 1 illustrates the appearance of IDDI over a period of 90 days. In case of DEX-PLGA implants, a significant change in appearance was observed only one day after incubation, with a pronounced initial increase in both length and diameter (Fig. 2). After reaching the maximum of expansion, they exhibited similar dimensions for approximately 50 days, followed by a subsequent decrease in both length and diameter. A maximum expansion in diameter (0.64 mm; 182 %) and in length (5.83 mm; 185 %) was noted. DEX-PEG-PLGA implants exhibited a gradual increase in both length and width. After 18 days, the implants showed complete expansion. The maximum expansion in diameter (0.62 mm; 178 %) was similar to DEX-PLGA implants. However, the increase in length (4.47 mm; 148 %) was surprisingly lower compared to DEX-PLGA implants. Despite the distinct initial phases, both formulations followed a comparable pattern and reverted to their initial dimensions around the 80-day mark. By day 104 at the latest, all IDDI had completely dissolved (data not shown).

Swelling presents a major concern for the potential damage to sensitive structures within the inner ear. Micro-computed tomography (μCT) imaging revealed sufficient space for the IDDI within the scala tympani, even in unswollen state and in combination with CI from different manufacturers [24]. Fig. 3A demonstrates that even a combination of swollen IDDI with a CI provides sufficient space in the human scala tympani. The schematic CI (orange cylinder) has a diameter of 0.8 mm, which is consistent with the typical basal diameters of CIs such as the MED-EL Flex 28, Cochlear Contour Advance, and Advanced Bionics HiFocus 1j [32]. However, studying swelling in the human cochlea under physiological conditions remains a considerable challenge. Consequently, the porcine model has recently gained more focus as a promising large animal model for human-like inner ear characteristics [33–35]. Although the scala tympani significantly and almost abruptly decreases in diameter at a distance of 15 mm from the round window membrane, co-administration appears still possible in the basal part (Fig. 3B). However, knowledge of segmented porcine cross-sectional data is limited and refers only to one publication [33]. Interindividual variations in geometry, as described for the human cochleae [36], must be considered.

Detailed investigations of the IDDI surface were conducted using SEM (Fig. 4). DEX-PLGA and DEX-PEG-PLGA implants were exposed to artificial perilymph over 28 days. The samples had to be dried before SEM analysis, resulting in discrepancies from moist conditions. DEX-PLGA implants revealed a significant surface alteration after only 3 days. The shrunken structures of DEX-PLGA implants resulted from drying, as the implants appeared smooth in the wetted state. PLGA is known for its bulk erosion, meaning the polymer undergoes degradation throughout its entire bulk volume, leading to a decrease in mass and structural integrity over time [37,38]. This type of erosion occurs uniformly throughout the material, as opposed to surface erosion where degradation occurs only at the surface. Li et al. described PLGA implants with a gel-like or hollow core after incubation in phosphate buffer saline but with still intact implant surfaces [39]. Applying vacuum to structures with a hollow core can lead to collapse or destruction of their internal structure. At day 28, DEX-PLGA implants were very fragile and no longer removable from buffer without destroying their nature. In contrast, the surface of DEX-PEG-PLGA implants remained intact until day 14. Defects on the surface were clearly visible at days 21 and 28. Overall, DEX-PEG-PLGA implants remained shape-stable and did not collapse compared to the DEX-PLGA counterpart. In some images, crystals on the surface were visible, mainly attributed to buffer salts

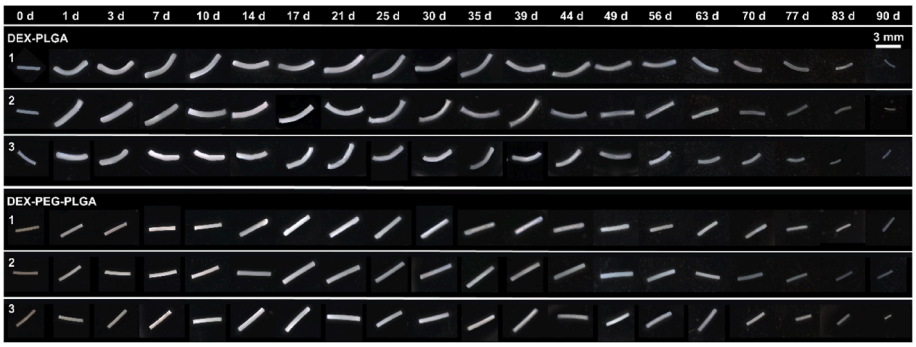

Fig. 1. Selected macroscopic images of DEX-PLGA and DEX-PEG-PLGA implants following exposure to artificial perilymph for 90 days, performed in triplicate. Scale bar on the top right.

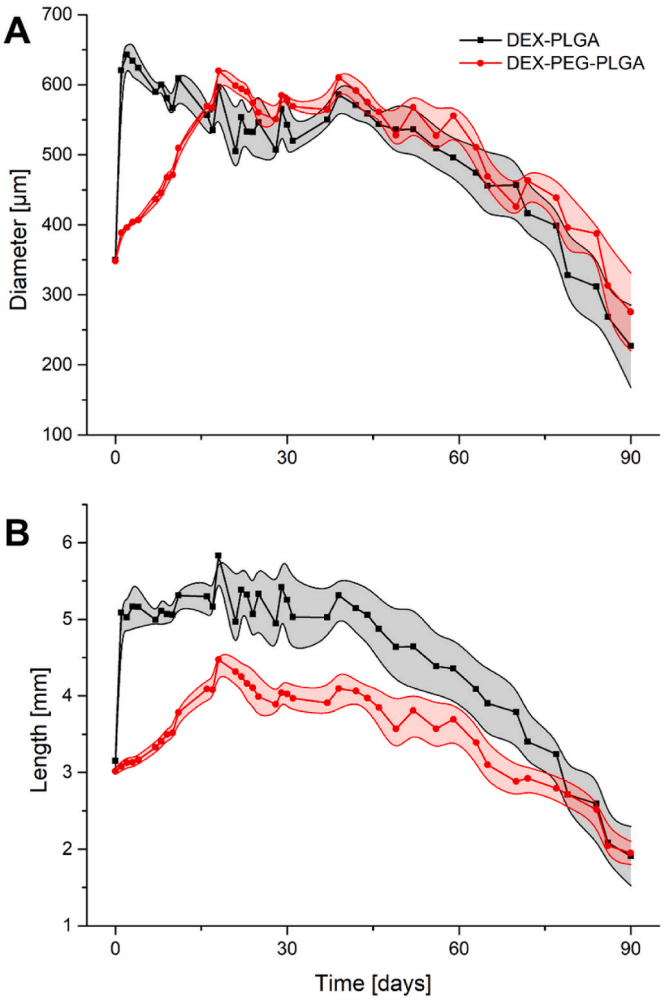

Fig. 2. Time-dependent changes in diameter (**A**) and length (**B**) of DEX-PLGA and DEX-PEG-PLGA implants following incubation in artificial perilymph at 37 °C. Data are presented as mean ± SD, n = 3.

determined by energy-dispersive X-ray spectroscopy (EDX; data not shown). Despite washing IDDI with double-distilled water after incubation, vacuum application led to the extraction of buffer salt crystals from inside the implants.

3.2. Water uptake and implant degradation

Aliphatic polyesters like PLGA and PEG-PLGA primarily undergo degradation through hydrolysis of the ester bonds linking lactic acid and glycolic acid. Upon reaching a certain molecular weight, the resulting oligomers become water-soluble and can diffuse out of the formulation, leading to measurable mass loss [40]. Since the hydrolysis of the ester bonds requires water, water uptake is a key factor to monitor. The absorption of water accelerates diffusion processes that influence both the mass loss of the water-soluble polymers and that of the drug. In relation to water uptake, we investigated the polymer degradation leading to polymer erosion. Degradation and erosion profiles of IDDI were determined by gravimetric analysis and GPC. Fig. 5A illustrates the water uptake behavior of IDDI. DEX-PLGA implants displayed rapid water uptake, reaching a plateau, and maintaining this level over time. This can be attributed to the incorporation of 10 % PEG, as PEG-free PLGA implants demonstrated a slow water uptake [28,41]. In contrast, DEX-PEG-PLGA implants displayed a different pattern, showing a gradual water uptake that peaked on day 21 and a significant rise in the overall amount of absorbed water. The matrix of DEX-PEG-PLGA implants might have a higher affinity for water binding, although it could exhibit lower swelling properties. This could be attributed to small amounts of residual PEG in the implants, which were not detected in the DSC analysis. PEG is known to enhance the water uptake of polylactic acid (PLA) nanoparticles [42]. In addition, DEX-PLGA implants exhibited significantly more pores and hollow structures (Fig. 4). These pores could result in lower water binding compared to their DEX-PEG-PLGA counterparts. The profiles of the two formulations corresponded to the optical changes of the IDDI. DEX-PLGA implants exhibited rapid water absorption and expansion. In contrast, DEX-PEG-PLGA showed delayed water uptake, with maximum complete enlargement occurring after 18 days. Unfortunately, the recording was limited to day 21 or 28, respectively, as the extraction and comprehensive analysis of the implants proved impractical thereafter due to their fragility. The observed water absorption and swelling align with the distinct release profiles identified by Lehner et al. [23] (Supplementary 1). DEX-PLGA implants demonstrated an initial release, whereas DEX-PEG-PLGA implants exhibited a phase with low drug release extending until day 12. These findings indicate a significant correlation between swelling kinetics and drug release profiles. Specifically, substantial drug release commenced only after the implants exhibited notable water uptake and expansion, aligning with observations by Bode et al. [43].

The rapid water uptake of DEX-PLGA implants played a crucial role in explaining their fast mass loss, which amounted to 48 % of the remaining mass after 14 days (Fig. 5B). In contrast, PEG-free implants exhibited significantly slower mass reduction [28,41]. The PLGA utilized in this study differs from that used in studies of Bassand et al. and Zlomke et al. However, PLGA polymers with similar labeled properties from different manufacturers exhibit a considerable degree of comparability [44,45]. In DEX-PLGA implants consisting of low molecular weight polymer chains (10.1 kDa; Fig. 5C), water-soluble oligomers were inherently present, causing an immediate decrease in mass as they

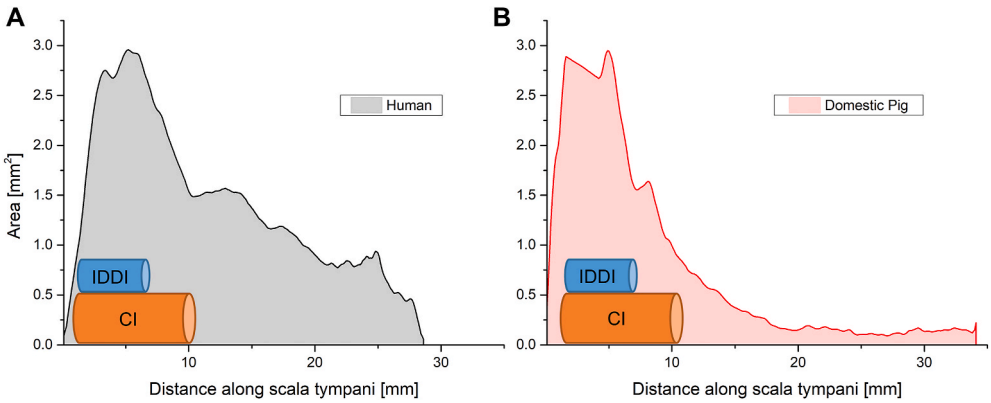

Fig. 3. Volume of the human (A) and porcine (B) scala tympani. The orange cylinder schematizes the basal part of a typical cochlear implant (CI) with a diameter of 0.8 mm. An intracochlear drug delivery implant (IDDI) at its maximum swelling state (0.64 × 5.83 mm) is shown as blue cylinder. The segmented cross-sectional data on various scala tympani structures were obtained from Fluidsim (Cochlear Fluids Simulator Version 4.08). (For interpretation of the references to colour in this figure legend, the reader is referred to the Web version of this article.)

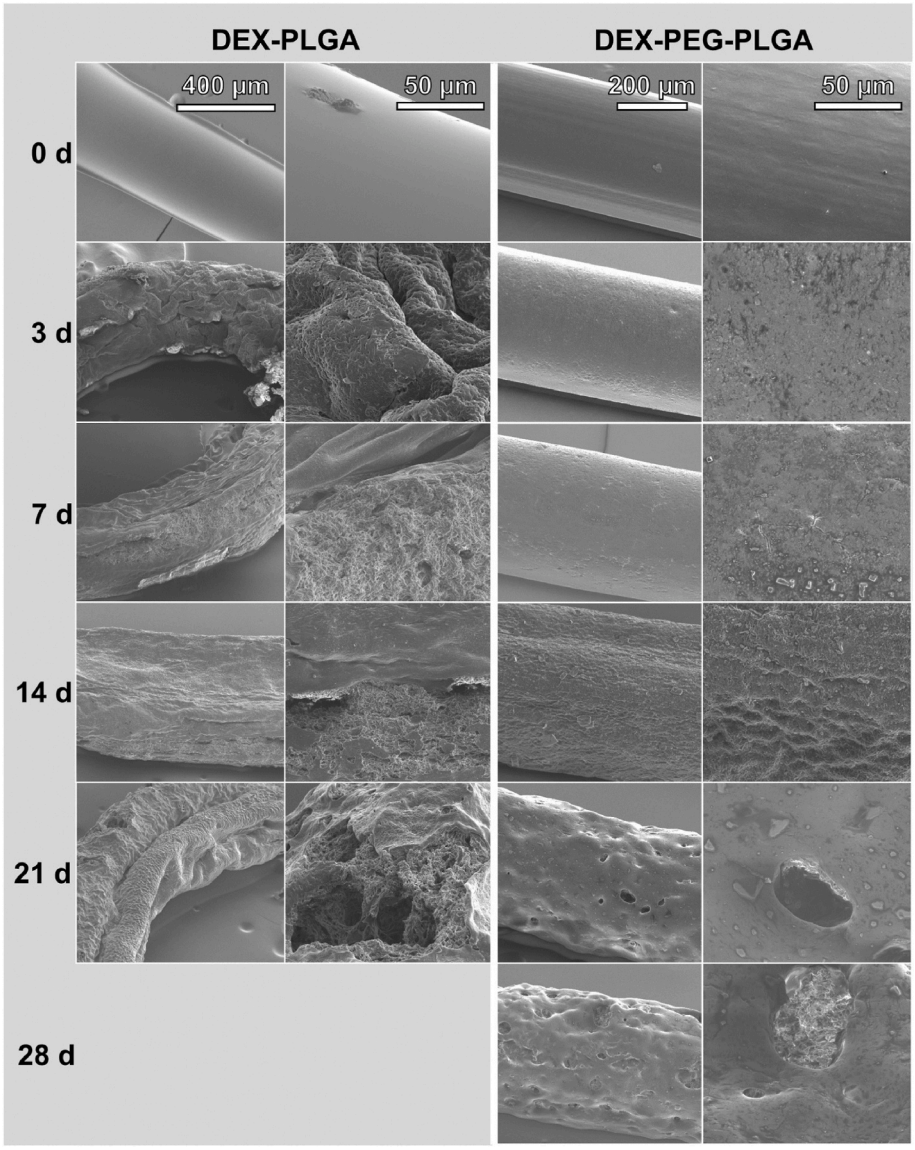

Fig. 4. Scanning electron microscopy images of surfaces of DEX-PLGA and DEX-PEG-PLGA implants before and after exposure to artificial perilymph at 37 °C for durations of 3, 7, 14, 21, and 28 days. By day 28, the DEX-PLGA implants had become too fragile to be removed for further analysis. Scale bars in the first images apply to the entire column.

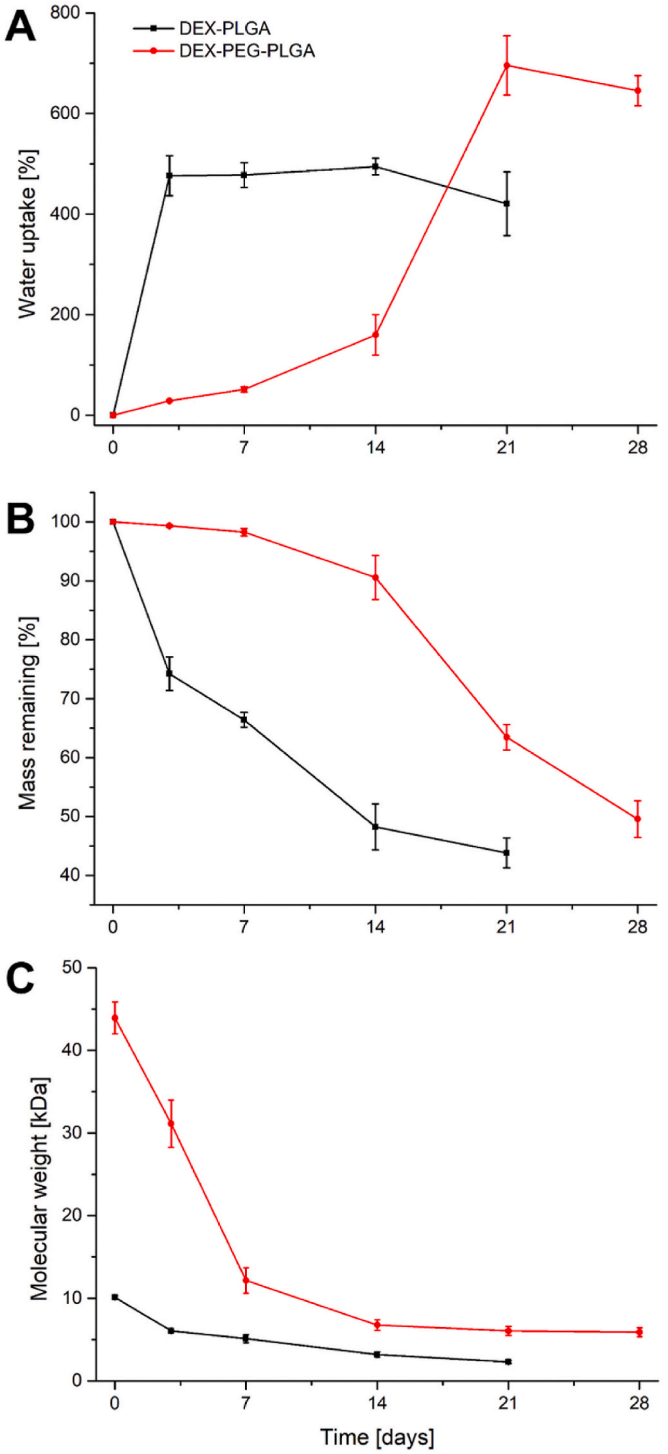

Fig. 5. The progress of water uptake (**A**) of IDDI, and the corresponding profiles of erosion (**B**) and degradation (**C**) during incubation in artificial perilymph at 37 °C. After 21 days, DEX-PLGA implants became too fragile for sample withdrawal. Data are presented as mean ± SD, n = 3.

rapidly diffuse out of the device. Additionally, this rapid decrease in mass could be attributed to the elimination of the highly water-soluble PEG 1500. In contrast to DEX-PEG-PLGA, PEG does not require cleavage from the PLGA chain and can therefore diffuse directly out of the matrix. DEX-PEG-PLGA implants retained 91 % of their mass after 14 days of incubation. This minor reduction can be attributed to low water uptake. Despite the initially low water uptake, substantial reduction of the molecular weight was observed in DEX-PEG-PLGA implants already after three days of incubation. The molecular weight decreased from 43.9 kDa to 12.2 kDa in the first 14 days. At that point, polymer chains may become water-soluble and can diffuse out of the device, resulting in a reduction in overall mass. Previous studies described that as soon as a critical polymer molecular weight is reached, important amounts of water penetrate into the system, leading to significantly increased drug release [43,46]. SEM images could confirm these findings, as minimal alteration of the IDDI surface could be observed until day 14 (Fig. 4). From day 21, however, an erosion of the surface became apparent. At this stage, the implant had absorbed the maximum amount of water creating a high diffusion gradient between the implant and the buffer solution, which facilitated the accelerated mass reduction. Similar results were described by de Souza et al. using PEG-PLGA from the same manufacturer [27].

3.3. *Differential scanning calorimetry*

IDDI were subjected to DSC measurements before and after incubation in artificial perilymph. Glass transition temperatures (T_g) of the dried samples were determined indicating morphological changes within the IDDI matrix. Complete drying of IDDI before measurement was crucial, as minimal water residues act as plasticizers and significantly lower the T_g [47]. Fig. 6 shows the DSC thermograms in the temperature range of the glass transitions between −20 °C and 70 °C. The fate of DEX-PLGA is shown in Fig. 6A. The incorporation of PEG 1500 lowers the T_g from 42.6 °C to 16.9 °C. After 3 days of incubation, the T_g increases to 37.9 °C. This increase is mainly attributed to rapid elimination of highly water-soluble PEG (serving as plasticizer) from the matrix due to fast water uptake (Fig. 5A). From day 7–21 post-incubation, T_gs around 40 °C close to the T_g of the raw polymer were determined. In general, the pattern between day 3 and 21 only varied marginally, as polymer degradation did not progress markedly between day 3 and day 21 (Fig. 5C).

The T_g of PEG-PLGA (23.1 °C) was significantly lower in its unprocessed state compared to the T_g of used PLGA. The incorporation of glucocorticoids itself had no effect on the T_g. Until day 14, the T_g continued to decrease (Fig. 6B). This is attributed to significant polymer degradation of the PLGA block (Fig. 5C). At day 21, the T_g abruptly increased to 36.1 °C. At this stage, ester cleavages had progressed to the point where PEG-PLGA chains became water-soluble and were subsequently eliminated. An overview of all T_g is shown in Table 2. In PEG-PLGA, PEG 6000 is covalently bound to the polymer. Consequently, the plasticizer can only be eliminated after cleavage of the ester bond between PLGA and PEG, or short-chained PEG-PLGA becomes water-soluble. When PEG was eliminated, it no longer contributed to lowering the T_g. In a recent study by de Souza et al., a decrease in PEG content was observed within the first 14 days using proton nuclear magnetic resonance spectroscopy (^{1}H NMR) [27]. After day 14, the PEG content remained unchanged. Unfortunately, de Souza et al. did not conduct DSC studies following an incubation period, which could have facilitated a more comprehensive comparison of the results.

Until now, the mechanism by which degradation products are eliminated from scala tympani *in vivo* remains unclear. Polymers with high molecular weight, such as fluorescein isothiocyanate (FITC)-dextran (4 kDa), exhibited significantly prolonged half-lives in the perilymph [35,48]. PLGA degrades via hydrolysis of the ester bonds between lactic acid and glycolic acid. However, PEG is not biodegradable and can remain in the perilymph for varying durations depending on its molecular weight. Therefore, a short-chain PEG was used as a plasticizer. PEGs with shorter chains than 1500 Da are paste-like or liquid, which increasingly complicating the extrusion process. In contrast, higher molecular weight PEGs could accumulate in the inner ear, posing a potential risk of ototoxicity. Unfortunately, PEG-PLGA polymers mainly with 5 kDa covalently bound PEG are commercially available (Sequens, Ashland, Evonik). A potential accumulation will be investigated in future studies.

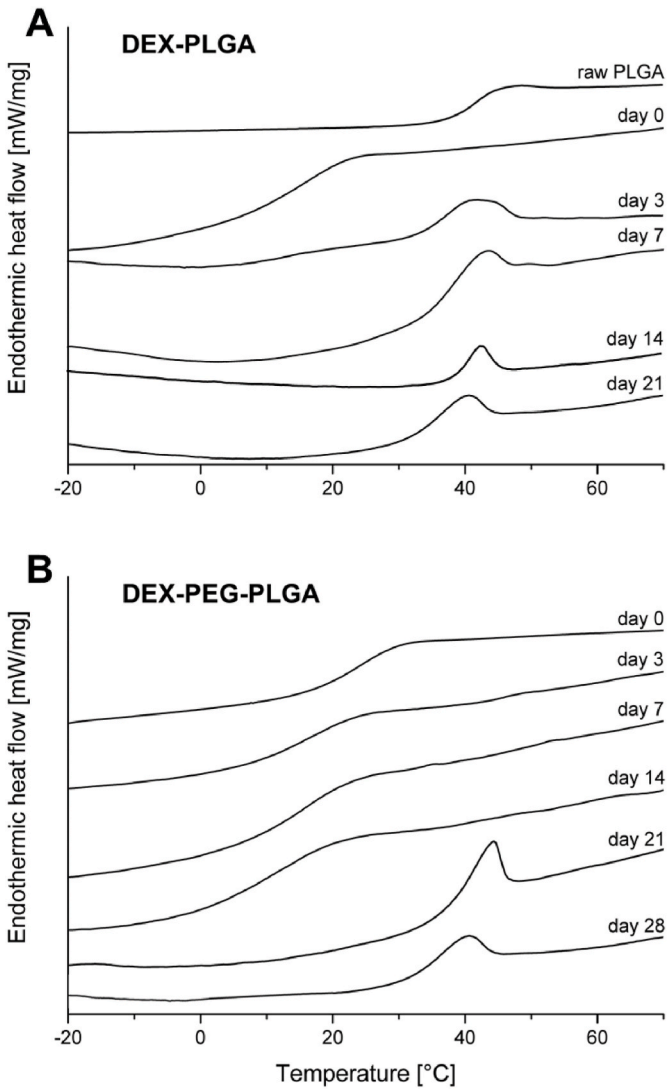

Fig. 6. DSC thermograms of dried DEX-PLGA (**A**) and DEX-PEG-PLGA (**B**) at selected time points after incubation in artificial perilymph at 37 °C. After 21 days, DEX-PLGA implants became too fragile for sample withdrawal. Measurements were carried out with a heating rate of 5 K/min. Glass transition temperatures of first heating cycles are displayed.

Table 2
Glass transition temperatures (T_g) of IDDI after incubation in artificial perilymph.

Time	T_g [°C]	
	DEX-PLGA	DEX-PEG-PLGA
day 0	16.9	24.3
day 3	37.3	16.4
day 7	39.7	14.7
day 14	40.2	11.8
day 21	36.1	39.2
day 28	not measured	36.4

3.4. Change in pH value of artificial perilymph

Polymer degradation of IDDI may have impact on the pH value of artificial perilymph with potential implications for physiological processes. While short-term pH reduction has been reported to have no physiological impact [49], prolonged acidification may lead to irreversible damage. *In vitro* experiments using the pH-sensitive fluorescence dye SNARF-1 were conducted to examine pH changes in artificial perilymph. Fig. 7A displays the emission spectra of SNARF-1 in artificial perilymph adjusted to various pH values. Spectra from 580 to 700 nm were measured using the green filter set, and the spectra from 660 to 700 nm were measured using the red filter set. As the pH value increases, the green spectrum undergoes a bathochromic shift, while the red spectrum exhibits heightened intensities. The best method for further pH calculation involved subtracting the intensity value at 682 nm (red filter set) from that measured at 606 nm (green filter set) and then dividing the result by the intensity value at 680 nm (green filter set). The pH-dependent ratios are illustrated in Fig. 7B. The Boltzmann plot served as the basis for all subsequent calculations. Reliable pH values could be derived from the emission intensity ratios obtained within the pH range spanning from pH 5.5 to pH 7.5 (Fig. 7B, black lines). This adjusted setup relates to *in vitro* and *in vivo* measurements using SNARF-4F [50].

1 mg of IDDI was placed in 100 μL of artificial perilymph. This ratio mirrored the proportion of a 0.35 × 3 mm IDDI (mass = 400 μg) within the perilymph of the human scala tympani (40 μg). For DEX-PLGA, a pH reduction of artificial perilymph to 6.49 was observed in the initial days (Fig. 8), supporting with the findings of the mass loss experiment (Fig. 5). A like explanation is that water-soluble acidic oligomers have passed into the perilymph thus lowering the pH. By day 7, the pH stabilized within the range of artificial perilymph (7.31 ± 0.03; blue bar). DEX-PEG-PLGA initially exhibited an unchanged pH, with a minimal decrease observed from day 14–21. During this period, the major change in mass reduction could be observed. Despite a major molecular weight reduction within the first days (Fig. 5C), no pH reduction was observed in this period. The decrease in pH during the first few days may increase the possibility of inner ear hair cell damage due to potential trauma from inserting a biodegradable IDDI into the scala tympani. An additional CI may increase potential hair cell damage, likely due to higher insertion trauma.

This method is suitable for measuring pH values of small volumes, even down to 1 μL, making it applicable for examining samples obtained through *in vivo* sequential perilymph sampling. In contrast to pH electrodes, a SNARF contaminated sample can also be used for pharmacokinetic measurements using HPLC-MS.

4. Conclusion

This study investigated the degradation behavior of intracochlear drug delivery implants (IDDI). Microscopy and SEM imaging revealed significant alterations in size and surface morphology of DEX-PLGA implants after only 3 days of exposure to artificial perilymph, while DEX-PEG-PLGA implants remained intact until day 14. Despite these morphological changes, the IDDIs could still be applicable in terms of cochlear dimensions in combination with cochlear implants (CI) in humans or in a domestic pig animal model. Gravimetric analysis and GPC demonstrated different degradation profiles between the two formulations, with DEX-PLGA implants exhibiting rapid water uptake and mass loss compared to DEX-PEG-PLGA implants. Furthermore, pH measurements showed a temporary decrease in pH in the initial days for DEX-PLGA implants, potentially attributed to the release of water-soluble acidic oligomers, while DEX-PEG-PLGA implants exhibited almost no pH changes during observation. Both formulations show promise for *in vivo* applications, although DEX-PEG-PLGA might hold a slight advantage. Overall, the study provides valuable insights into the degradation behavior of IDDI, which can be used for the development and optimization of such implants for controlled inner ear drug release. Future studies must also focus on *in vivo* pH measurements and the detection of degradation products in guinea pigs or domestic pigs.

Formatting of funding sources

This research did not receive any specific grant from funding

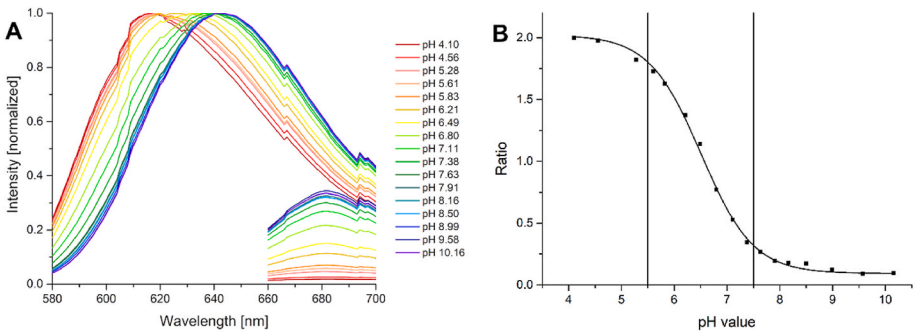

Fig. 7. (**A**) Fluorescence spectra of SNARF-1 in artificial perilymph as function of pH value. (**B**) Calculated ratios from the fluorescence spectra fitted with Boltzmann plot and limits of reliable pH calculation (vertically black lines at pH 5.5 and pH 7.5).

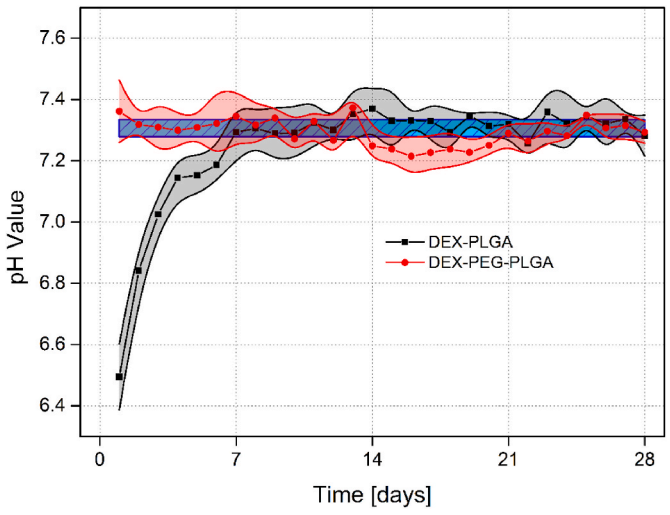

Fig. 8. Time-dependent pH change of artificial perilymph induced by PLGA degradation of IDDI. The blue bar represents the pH value of untreated artificial perilymph. Data are presented as mean ± SD, n = 3. (For interpretation of the references to colour in this figure legend, the reader is referred to the Web version of this article.)

agencies in the public, commercial, or not-for-profit sectors.

CRediT authorship contribution statement

Eric Lehner: Writing – original draft, Visualization, Methodology, Investigation, Formal analysis, Conceptualization. **Arne Liebau:** Writing – review & editing, Methodology, Investigation, Conceptualization. **Matthias Menzel:** Writing – original draft, Visualization, Investigation, Formal analysis. **Christian E.H. Schmelzer:** Writing – review & editing, Resources, Conceptualization. **Wolfgang Knolle:** Writing – original draft, Investigation, Formal analysis. **Jonas Scheffler:** Writing – review & editing, Investigation, Formal analysis. **Wolfgang H. Binder:** Writing – review & editing, Methodology, Investigation, Formal analysis. **Stefan K. Plontke:** Writing – review & editing, Supervision, Resources, Conceptualization. **Karsten Mäder:** Writing – review & editing, Supervision, Resources, Conceptualization.

Declaration of competing interest

The authors declare that they have no known competing financial interests or personal relationships that could have appeared to influence the work reported in this paper.

Data availability

Data will be made available on request.

Acknowledgments

We appreciate the assistance provided by Dr. Joana Heinzelmann from the Department of Ophthalmology, Martin Luther University Halle-Wittenberg, in conducting light microscopic measurements.

Appendix A. Supplementary data

Supplementary data to this article can be found online at https://doi.org/10.1016/j.jddst.2024.105972.

References

[1] A.N. Salt, K. Hirose, Communication pathways to and from the inner ear and their contributions to drug delivery, Hear. Res. 362 (2018) 25–37, https://doi.org/10.1016/J.HEARES.2017.12.010.
[2] J. Devare, S. Gubbels, Y. Raphael, Outlook and future of inner ear therapy, Hear. Res. 368 (2018) 127–135, https://doi.org/10.1016/j.heares.2018.05.009.
[3] S.K. Plontke, G. Götze, T. Rahne, A. Liebau, Intracochlear drug delivery in combination with cochlear implants: Current aspects, HNO 65 (2017) 19–28, https://doi.org/10.1007/s00106-016-0285-9.
[4] B. Szeto, H. Chiang, C. Valentini, M. Yu, J.W. Kysar, A.K. Lalwani, Inner ear delivery : Challenges and opportunities, Laryngoscope Investig Otolaryngol 5 (2020) 122–131, https://doi.org/10.1002/lio2.336.
[5] S.K. Plontke, M. Girndt, C. Meisner, I. Fischer, I. Böselt, J. Löhler, B. Ludwig-Kraus, M. Richter, J. Steighardt, B. Reuter, C. Böttcher, J. Langer, W. Pethe, I. Seiwerth, N. Jovanovic, W. Großmann, A. Kienle-Gogolok, A. Boehm, M. Neudert, M. Diensthuber, A. Müller, S. Dazert, O. Guntinas-Lichius, J. Hornung, V. Vielsmeier, J. Stadler, T. Rahne, High-dose glucocorticoids for the Treatment of sudden hearing loss, NEJM Evidence 3 (2024), https://doi.org/10.1056/EVIDoa2300172.
[6] K.S. Alzamil, F.H. Linthicum, Extraneous round window membranes and plugs: possible effect on intratympanic therapy, Ann. Otol. Rhinol. Laryngol. 109 (2000) 30–32, https://doi.org/10.1177/000348940010900105.
[7] H. Hahn, B. Kammerer, A. DiMauro, A.N. Salt, S.K. Plontke, Cochlear microdialysis for quantification of dexamethasone and fluorescein entry into scala tympani during round window administration, Hear. Res. 212 (2006) 236–244, https://doi.org/10.1016/J.HEARES.2005.12.001.
[8] M. Gehrke, J. Verin, D. Gnansia, G. Tourrel, M. Risoud, C. Vincent, F. Siepmann, J. Siepmann, Hybrid Ear Cubes for local controlled dexamethasone delivery to the inner ear, Eur. J. Pharmaceut. Sci. 126 (2019) 23–32, https://doi.org/10.1016/j.ejps.2018.04.045.
[9] E. Lehner, A. Liebau, F. Syrowatka, W. Knolle, S.K. Plontke, K. Mäder, Novel biodegradable Round Window Disks for inner ear delivery of dexamethasone, Int J Pharm 594 (2021) 120180, https://doi.org/10.1016/j.ijpharm.2020.120180.
[10] K. Mäder, E. Lehner, A. Liebau, S.K. Plontke, Controlled drug release to the inner ear: Concepts, materials, mechanisms, and performance, Hear. Res. 368 (2018) 49–66, https://doi.org/10.1016/J.HEARES.2018.03.006.
[11] R. Mau, T. Eickner, G. Jüttner, Z. Gao, C. Wei, N. Fiedler, V. Senz, T. Lenarz, N. Grabow, V. Scheper, H. Seitz, Micro injection Molding of drug-Loaded round window Niche implants for an animal model using 3D-Printed Molds, Pharmaceutics 15 (2023), https://doi.org/10.3390/pharmaceutics15061584.
[12] C. Rathnam, S.T.D. Chueng, Y.L.M. Ying, K.B. Lee, K. Kwan, Developments in Bio-Inspired nanomaterials for Therapeutic delivery to treat hearing loss, Front. Cell. Neurosci. 13 (2019) 493, https://doi.org/10.3389/FNCEL.2019.00493/BIBTEX.

[13] A.N. Salt, S.K. Plontke, Pharmacokinetic principles in the inner ear: influence of drug properties on intratympanic applications, Hear. Res. 368 (2018) 28–40, https://doi.org/10.1016/J.HEARES.2018.03.002.
[14] R. Briggs, S. O 'Leary, C. Birman, K. Plant, R. English, P. Dawson, F. Risi, J. Gavrilis, K. Needham, R. Cowan, Comparison of electrode impedance measures between a dexamethasone-eluting and standard Cochlear™ Contour Advance® electrode in adult cochlear implant recipients, Hear. Res. 390 (2020) 107924, https://doi.org/10.1016/j.heares.2020.107924.
[15] A.A. Eshraghi, A. Wolfovitz, R. Yilmazer, C. Garnham, A.B. Yilmazer, E. Bas, P. Ashman, J. Roell, J. Bohorquez, R. Mittal, R. Hessler, D. Sieber, J. Mittal, Otoprotection to implanted cochlea exposed to Noise trauma with dexamethasone eluting electrode, Front. Cell. Neurosci. 13 (2019), https://doi.org/10.3389/FNCEL.2019.00492.
[16] A. Liebau, S. Schilp, K. Mugridge, I. Schön, M. Kather, B. Kammerer, J. Tillein, S. Braun, S.K. Plontke, Long-term in vivo release profile of dexamethasone-Loaded Silicone Rods implanted into the cochlea of Guinea pigs, Front. Neurol. 10 (2020), https://doi.org/10.3389/FNEUR.2019.01377.
[17] R. Manrique-Huarte, C. Zulueta-Santos, D. Calavia, M.Á. De Linera-Alperi, M. A. Gallego, C. Jolly, M. Manrique, Cochlear implantation with a dexamethasone eluting electrode array: Functional and Anatomical changes in Non-human Primates, Otol. Neurotol. 41 (2020) e812–e822, https://doi.org/10.1097/MAO.0000000000002686.
[18] E. Simoni, E. Gentilin, M. Candito, G. Borile, F. Romanato, M. Chicca, S. Nordio, M. Aspidistria, A. Martini, D. Cazzador, L. Astolfi, Immune response after cochlear implantation, Front. Neurol. 11 (2020) 341, https://doi.org/10.3389/FNEUR.2020.00341.
[19] D. Chen, Y. Luo, J. Pan, A. Chen, D. Ma, M. Xu, J. Tang, H. Zhang, Long-term release of dexamethasone with a Polycaprolactone-coated electrode Alleviates fibrosis in cochlear implantation, Front. Cell Dev. Biol. 9 (2021) 2948, https://doi.org/10.3389/FCELL.2021.740576/BIBTEX.
[20] E. Pierstorff, S. Chen, M.P. Chaparro, J.M. Cortez, Y.J. Chen, S.Y. Ryu, S.M. Tsai, M. M. Baum, W.W. Yang, F. Kalinec, T. Smith, S. Ludwig, W.H. Slattery, A polymer-based extended release system for stable, long-term intracochlear drug delivery, Otol. Neurotol. 39 (2018) 1195–1202, https://doi.org/10.1097/MAO.0000000000001977.
[21] S.K. Plontke, A. Liebau, E. Lehner, D. Bethmann, K. Mäder, T. Rahne, Safety and audiological outcome in a case series of tertiary therapy of sudden hearing loss with a biodegradable drug delivery implant for controlled release of dexamethasone to the inner ear, Front. Neurosci. 16 (2022), https://doi.org/10.3389/fnins.2022.892777.
[22] E. Lehner, D. Gündel, A. Liebau, S.K. Plontke, K. Mäder, Intracochlear PLGA based implants for dexamethasone release: Challenges and solutions, Int J Pharm X (2019) 1, https://doi.org/10.1016/j.ijpx.2019.100015.
[23] E. Lehner, C. Honeder, W. Knolle, W. Binder, J. Scheffler, S.K. Plontke, A. Liebau, K. Mäder, Towards the optimization of drug delivery to the cochlear apex: influence of polymer and drug selection in biodegradable intracochlear implants, Int J Pharm 643 (2023), https://doi.org/10.1016/j.ijpharm.2023.123268.
[24] E. Lehner, M. Menzel, D. Gündel, S.K. Plontke, K. Mäder, J. Klehm, H. Kielstein, A. Liebau, Microimaging of a novel intracochlear drug delivery device in combination with cochlear implants in the human inner ear, Drug Deliv Transl Res 12 (2022) 257–266, https://doi.org/10.1007/S13346-021-00914-9.
[25] C. Witt, K. Mäder, T. Kissel, The degradation, swelling and erosion properties of biodegradable implants prepared by extrusion or compression moulding of poly (lactide-co-glycolide) and ABA triblock copolymers, Biomaterials 21 (2000) 931–938, https://doi.org/10.1016/S0142-9612(99)00262-8.
[26] V. Milacic, S.P. Schwendeman, Lysozyme release and polymer erosion behavior of injectable implants prepared from plga-peg block copolymers and plga/plga-peg blends, Pharm. Res. (N. Y.) 31 (2014) 436–448, https://doi.org/10.1007/s11095-013-1173-6.
[27] L.E. de Souza, R. Eckenstaler, F. Syrowatka, M. Beck-Broichsitter, R.A. Benndorf, K. Mäder, Has PEG-PLGA advantages for the delivery of hydrophobic drugs? Risperidone as an example, J. Drug Deliv. Sci. Technol. 61 (2021) 102239, https://doi.org/10.1016/j.jddst.2020.102239.
[28] C. Bassand, J. Freitag, L. Benabed, J. Verin, F. Siepmann, J. Siepmann, PLGA implants for controlled drug release: impact of the diameter, Eur. J. Pharm. Biopharm. 177 (2022) 50–60, https://doi.org/10.1016/J.EJPB.2022.05.020.
[29] S. Leisz, M.L. Trutschel, K. Mäder, C. Scheller, C. Strauss, S. Simmermacher, Tabotamp®, respectively, Surgicel®, increases the cell death of neuronal and glial cells in vitro, Materials 13 (2020), https://doi.org/10.3390/ma13112453.
[30] J. Strätz, A. Liedmann, M.L. Trutschel, K. Mäder, T. Groth, S. Fischer, Development of hydrogels based on oxidized cellulose sulfates and carboxymethyl chitosan, Cellulose 26 (2019) 7371–7382, https://doi.org/10.1007/S10570-019-02596-6/FIGURES/9.
[31] K.J. Buckler, R.D. Vaughan-Jones, Application of a new pH-sensitive fluoroprobe (carboxy-SNARF-1) for intracellular pH measurement in small, isolated cells, Pflügers Archiv 417 (2 417) (1990) 234–239, https://doi.org/10.1007/BF00370705, 1990.
[32] Y.N. Ertas, D. Ozpolat, S.N. Karasu, N. Ashammakhi, Recent Advances in cochlear implant electrode array Design Parameters, Micromachines 13 (2022), https://doi.org/10.3390/mi13071081.
[33] A. Moatti, S. Connard, N. De Britto, W.A. Dunn, S. Rastogi, M. Rai, L.V. Schnabel, F. S. Ligler, K.A. Hutson, D.C. Fitzpatrick, A. Salt, C.J. Zdanski, A. Greenbaum, Surgical procedure of intratympanic injection and inner ear pharmacokinetics simulation in domestic pigs, Front. Pharmacol. 15 (2024), https://doi.org/10.3389/fphar.2024.1348172.
[34] E. Yildiz, M. Gerlitz, A.J. Gadenstaetter, L.D. Landegger, M. Nieratschker, D. Schum, M. Schmied, A. Haase, F. Kanz, A.M. Kramer, R. Glueckert, H. Staecker, C. Honeder, C. Arnoldner, Single-incision cochlear implantation and hearing evaluation in piglets and minipigs, Hear. Res. 426 (2022), https://doi.org/10.1016/j.heares.2022.108644.
[35] E. Yildiz, A.J. Gadenstaetter, M. Gerlitz, L.D. Landegger, R. Liepins, M. Nieratschker, R. Glueckert, H. Staecker, C. Honeder, C. Arnoldner, Investigation of inner ear drug delivery with a cochlear catheter in piglets as a representative model for human cochlear pharmacokinetics, Front. Pharmacol. 14 (2023), https://doi.org/10.3389/fphar.2023.1062379.
[36] R. Hussain, A. Frater, R. Calixto, C. Karoui, J. Margeta, Z. Wang, M. Hoen, H. Delingette, F. Patou, C. Raffaelli, C. Vandersteen, N. Guevara, Anatomical variations of the human cochlea using an image analysis tool, J. Clin. Med. 12 (2023), https://doi.org/10.3390/jcm12020509.
[37] A. Göpferich, Polymer bulk erosion, Macromolecules 30 (1997) 2598–2604, https://doi.org/10.1021/ma961627y.
[38] F. Von Burkersroda, L. Schedl, A. Göpferich, Why Degradable Polymers Undergo Surface Erosion or Bulk Erosion, 2002.
[39] S.M. Li, H. Garreau, M. Vert, Structure-property Relationships in the Case of the Degradation of Massive Poly(-Hydroxy Acids) in Aqueous Media, 1990.
[40] T.G. Park, Degradation of poly(d,l-lactic acid) microspheres: effect of molecular weight, J. Contr. Release 30 (1994) 161–173, https://doi.org/10.1016/0168-3659(94)90263-1.
[41] C. Zlomke, M. Barth, K. Mäder, Polymer degradation induced drug precipitation in PLGA implants – Why less is sometimes more, Eur. J. Pharm. Biopharm. 139 (2019) 142–152, https://doi.org/10.1016/J.EJPB.2019.03.016.
[42] P. Quellec, R. Gref, L. Perrin, E. Dellacherie, F. Sommer, J.M. Verbavatz, M. J. Alonso, Protein encapsulation within polyethylene glycol-coated nanospheres. I. Physicochemical characterization, J. Biomed. Mater. Res. 42 (1998) 45–54, https://doi.org/10.1002/(SICI)1097-4636(199810)42:1<45::AID-JBM7>3.0.CO;2-O.
[43] C. Bode, H. Kranz, A. Fivez, F. Siepmann, J. Siepmann, Often neglected: PLGA/PLA swelling orchestrates drug release: HME implants, J. Contr. Release 306 (2019) 97–107, https://doi.org/10.1016/j.jconrel.2019.05.039.
[44] J. Sun, J. Walker, M. Beck-Broichsitter, S.P. Schwendeman, Characterization of commercial PLGAs by NMR spectroscopy, Drug Deliv Transl Res 12 (2022) 720–729, https://doi.org/10.1007/s13346-021-01023-3.
[45] J. Walker, J. Albert, D. Liang, J. Sun, R. Schutzman, R. Kumar, C. White, M. Beck-Broichsitter, S.P. Schwendeman, In vitro degradation and erosion behavior of commercial PLGAs used for controlled drug delivery, Drug Deliv Transl Res 13 (2023) 237–251, https://doi.org/10.1007/s13346-022-01177-8.
[46] H. Gasmi, J.F. Willart, F. Danede, M.C. Hamoudi, J. Siepmann, F. Siepmann, Importance of PLGA microparticle swelling for the control of prilocaine release, J. Drug Deliv. Sci. Technol. 30 (2015) 123–132, https://doi.org/10.1016/j.jddst.2015.10.009.
[47] P. Blasi, S.S. D'Souza, F. Selmin, P.P. DeLuca, Plasticizing effect of water on poly (lactide-co-glycolide), J. Contr. Release 108 (2005) 1–9, https://doi.org/10.1016/j.jconrel.2005.07.009.
[48] A.N. Salt, R.M. Gill, J.J. Hartsock, Perilymph kinetics of FITC-dextran Reveals Homeostasis Dominated by the cochlear Aqueduct and Cerebrospinal fluid, JARO J. Assoc. Res. Otolaryngol. 16 (2015) 357–371, https://doi.org/10.1007/s10162-015-0512-1.
[49] F. Tanaka, C.A. Whitworth, L.P. Rybak, Influence of pH on the ototoxicity of cisplatin: a round window application study, Hear. Res. 177 (2003) 21–31, https://doi.org/10.1016/S0378-5955(02)00771-2.
[50] A. Schädlich, S. Kempe, K. Mäder, Non-invasive in vivo characterization of microclimate pH inside in situ forming PLGA implants using multispectral fluorescence imaging, J. Contr. Release 179 (2014) 52–62, https://doi.org/10.1016/j.jconrel.2014.01.024.